

ADAPTIVE POLE-ZERO CANCELLATION IN GRINDING FORCE CONTROL

PART I: REAL-TIME ESTIMATION

Hodge E. Jenkins¹

Georgia Institute of Technology
The George W. Woodruff School
of Mechanical Engineering
Atlanta, GA 30332-0405

Thomas R. Kurfess

Georgia Institute of Technology
The George W. Woodruff School
of Mechanical Engineering
Atlanta, GA 30332-0405

ABSTRACT

To achieve cost-effective, high quality precision parts, it is important to determine grinding process dynamics and subsequently control the process. A time-varying grinding process model is needed to provide an adaptive, robust controller design appropriate for creating precision surfaces in a timely manner. To this end, a real-time process model relating the material removal rate to measurable process attributes is established and optimized using multiple input sources. The resulting real-time model is superior to fixed parameter grinding models in terms of calculating material removal. An adaptive pole-zero cancellation (inverse grinding dynamics) technique is developed to reduce the effects of the grinding process variation for force control.

The implementation of this adaptive estimation and control approach in surface (traverse) grinding provides a superior surface following capability for fine finishing, as compared to fixed gain controllers. The adaptively controlled grinding system also demonstrates an ability to provide stable, fast force regulation with less variation than conventional controllers. This is critical in providing force control for use in the reduction of processing time. The focus of this research is primarily the grinding of steels. The research is presented in two parts: Part I: real-time estimation and Part II: adaptive control.

BACKGROUND

Grinding is an extensively used and important machining operation, that has been stated to account for a significant percentage (20%) of all machining costs in the industrialized world (Malkin, 1989). As the number of precision designed products increases, the application of grinding will only increase accordingly.

¹ Author is presently with Lucent Technologies in Norcross, GA.

Quality and production of precision parts are directly impacted by the ability of the grinding process control. In typical industrial grinders only position and feed velocity are controlled; force control is not implemented. Previous attempts at fixed-gain, force control systems have been found to be of limited use because of process variation (Tonshoff, 1986). Indeed, a fixed-parameter controller may even lead to instability and to damage. A time-varying grinding process model is needed to provide an adaptive, robust controller design appropriate for creating precision surfaces in a timely manner.

There are several advantages of a force-controlled grinding system. Without force control there is a trade-off between spark-out time and residual error in the ground part. Under force control a force trajectory can be followed to reduce the spark-out time. The positional error can be reduced by providing a constant and repeatable force which translates into dimensional accuracy and repeatability from part to part.

Current industrial grinding practice is to use slow feedrates in the transition between roughing and fine finishing. In roughing relatively large feedrates (and forces) are applied to remove large amounts of material. A time delay between roughing and fine finishing, where the feedrate is zero, allows a reduction of force to occur. This tarying time is a fixed amount of time with no assurances of the desired force reduction. By controlling the force, dimensional variations and damage could be limited during roughing as well as reducing in the tarying time.

The outcome of this research is a real-time model with multi-sensor estimation implemented in an adaptive force control scheme to maintain a high MRR and limit forces with changing process parameters. The system achieves a stable force control with high fidelity for use in reducing cycle time and greater surface following capability for fine finishing. A schematic of the resulting system developed in this research is presented in Figure 1.

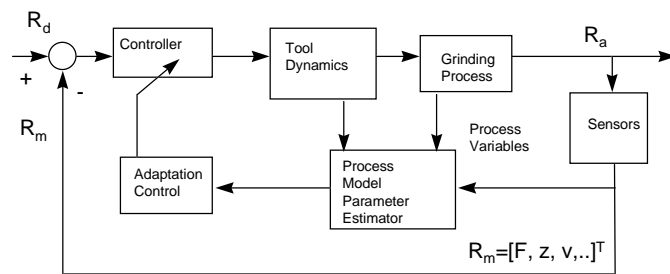


Figure 1. Adaptive Estimation and Control Schematic.

GRINDING PROCESS MODELS

The variable nature of the grinding process has been linked to the physical descriptions of the actions between the grits with the workpiece. Grinding is a complex operation, seen as three separate and concurrent process actions: (1) cutting, (2) plowing, and (3) rubbing (Hahn and Lindsay 1971, Samuels 1978, Salmon 1992). In general, all three grinding process actions occur simultaneously in varying distributions depending on the grinding wheel, material, and operating conditions, making detailed process analysis, modeling and control difficult.

Previous work has demonstrated that grinding is a time-varying process and should be modeled in real-time (Jenkins, Kurfess and Ludwick, 1996). The empirical grinding process model selected in this research is based on a combination of the grinding model developed by Hahn and Lindsay as well as the Preston model provided previously (Jenkins, et al, 1996). It should be noted that although Preston's original work was related to abrasive machining and polishing of optics, the model used in this work is similar to the model formulation of Hahn and Lindsay, Malkin, Coes, as well as others. The selected, two-parameter grinding model is given below in equation (1). Its validity has been previously demonstrated.

$$Q = K_p(F_N - F_{TH})V; \quad F_N \geq F_{TH} \quad (1)$$

In this equation, the material removal rate is defined as Q , while F_N is the applied normal force. The threshold normal force, F_{TH} , is the lower limit of the normal force below which no significant amount of material removal takes place. V is the surface speed of the grinding wheel. The coefficient, K_p , and the threshold force, F_{TH} , in this model are determined experimentally. These coefficients represent the current condition of the specific grinding wheel and workpiece. Thus, calculations to separate rubbing, plowing, and cutting effects of the process are not needed.

For plunge grinding, the material removal rate, Q , can be expressed as the product of the grinding contact area (A) and the grinding wheel feed velocity (\dot{x}_f).

$$Q = \dot{x}_f A \quad (2)$$

Combining equations (1) and (2), the wheel feed velocity is written to relate the normal force to the grinding wheel feed velocity as:

$$F_N - F_{TH} = \dot{x}_f \frac{A}{K_p V} \quad (3)$$

Upon examining equation (3), it should be apparent that the grinding process may be thought of as damping. Indeed, the feedrate (velocity), \dot{x}_f , of the grinding wheel through the part is linearly

related to the normal force, F_N (minus the threshold force), assuming that part and grinding wheel remain in contact. This is compatible with the physical observations of the process.

A block diagram of the grinding process based on equation (1) is seen in the exploded view of the process in the lower section of Figure 2. Here the relationship between the measured output of the position loop, (the encoder position, x_e) and the actual ground surface position, x_f , for a plunge grinding is seen. Note the interaction between the servo controlled position measurement, x_e , and the workpiece may be thought of as a spring, K_S . It can be readily seen from examining Figure 2, that the grinding process affects the overall system response and any attempt to control the grinding normal force.

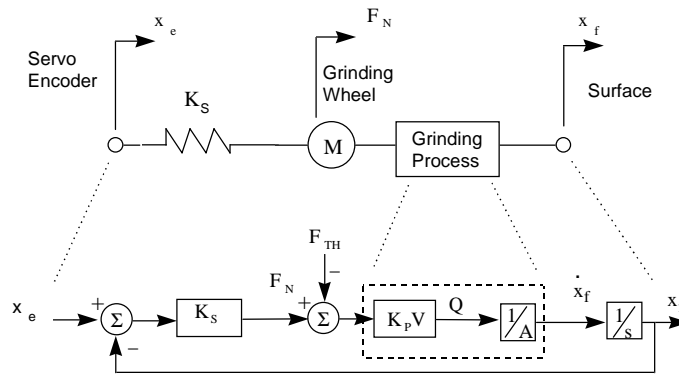


Figure 2. Block Diagram of Model of the System with the Grinding Process.

GRINDING MODEL PARAMETER IDENTIFICATION

The model parameters, F_{TH} and K_P , of equation (1) are identified by conducting position controlled grinding experiments and force controlled grinding experiments. The mathematical basis for identification in both types of experiments as previously outlined (Jenkins, et al, 1996). The response of the grinding wheel, $x_f(t)$, to the position step input of magnitude (X_e), described by equation (4).

$$x_f(t) = X_e \left(1 - e^{-(K_P K_S V/A)t} \right) \quad (4)$$

The exponent, $(K_P K_S V/A)$, of equation (4) is estimated from experiments off-line by the use of an auto-regressive, least squares parameter estimation technique (ARX, Ljung 1987).

In another series of experiments the normal force, F_N , is maintained at constant levels to determine K_P and F_{TH} . A fixed-gain controller is used for these experiments. From equation (1) it can be seen that maintaining a constant normal grinding force (along with constant surface

speed and contact area) results in a constant MRR. Thus an average value of the coefficient, K_P , may be experimentally found by achieving a near-constant normal grinding force and rewriting equation (1) to the following form.

$$K_P = \frac{\dot{x}_f A}{(F_N - F_{TH})V} \quad (5)$$

Fixed Parameter Model Performance

Table 1 lists the average resulting values for model coefficient, K_P , and the threshold force, F_{TH} , for the all the materials tested in the plunge grinding experiments. Overall, the values for grinding model coefficient ranged between $43.3 \times 10^{-6} \text{-mm}^2/\text{N}$ for the softest material tested and $3.4 \times 10^{-6} \text{ mm}^2/\text{N}$ for Inconel 718. As expected the harder materials have the lower coefficients, except for the case of the Inconel 718 which has a higher fracture toughness than the carbon steels tested. A significant result of these experiments is that the threshold normal force is similar in all cases (F_{TH} varied from 11.3 N to 13.1 N). The parameter variations of K_P and F_{TH} are seen by the standard deviations. The standard deviation of K_P is as large as 50% of the mean, while the threshold force standard deviation is generally within 20%. Clearly K_P is the most important parameter to determine in real-time.

Table 1. Identified Grinding Model Parameters.

Material	Mean Model Coefficient K_P ($10^{-6} \text{ mm}^2/\text{N}$)	Std. Dev. Model Coefficient K_P ($10^{-6} \text{ mm}^2/\text{N}$)	Mean Threshold Force, F_{TH} (N) normalized to 36-mm^2 area	Std. Dev. Threshold Force F_{TH} (N)
AISI 8119	6.3	3.5	11.3	2.1
Inconel 718	3.4	1.8	11.3	2.8
AISI 4142	8.0	4.4	13.1	2.7
AISI A-2	8.3	3.9	12.4	2.8
AISI O-1	10.7	2.7	12.5	4.7
AISI 1020	44.3	10.7	12.7	1.3

The effect of the threshold force variation on the estimated value of K_P is also examined by varying the threshold force, determining K_P , simulating the grinding, and calculating the model error covariance. Thus, a sensitivity analysis based on 20% variation on the F_{TH} value. It is interesting to note that the F_{TH} variation produces little change (1% to 7%) in the resulting grinding model error covariance. This is because of the offsetting effects of changes in K_P and $F_N - F_{TH}$, which are both used in the calculation of the grinder displacements.

Force Control Grinding Simulations Fixed Model

Force regulated grinding experiments are simulated using MATLAB scripts for the model of equation (1) and the recorded experimental data. Figure 3 shows typical grinder displacements and the response of the process model to the normal force for specific experiments. The simulations reveal that when the coefficient, K_P , is held constant, the estimated grinder position and the resulting part surface geometry quickly diverge from the actual experimental data as seen in Figure 5 for a typical constant force, plunge grind. K_P is seen as valid only over short intervals of time (1 to 2 seconds).

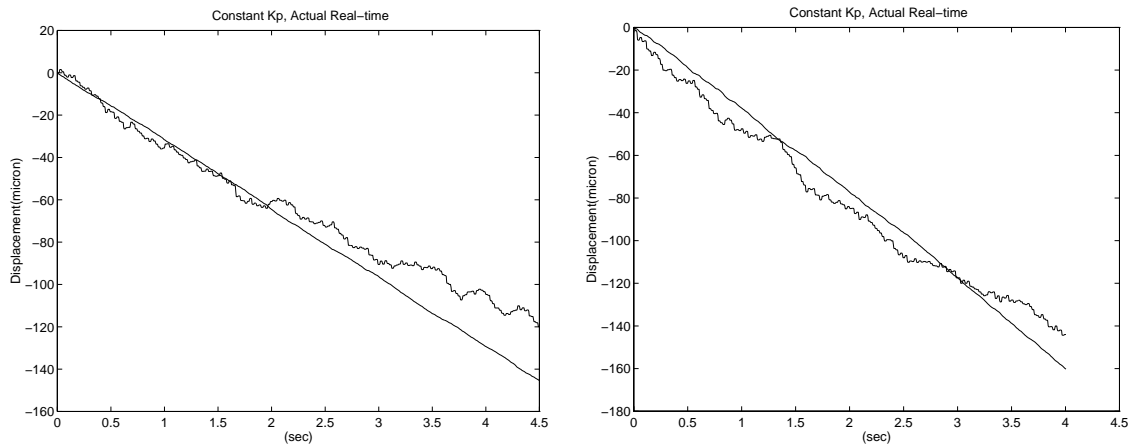


Figure 3. Grinder Displacements : Actual and Simulation Under Force Regulation AISI 1020.

Real-Time Parameter Estimation Approach

If the grinding model parameters can be frequently updated, the long-term accuracy of the model should be improved. Thus, real-time estimation of K_P is applied. The first attempt at this is to calculate the coefficient in real-time and use low-pass filtering to remove numerical differentiation noise. Data from the previous force controlled grinding experiments are used as the basis for the evaluations of the real-time, parameter estimations.

The calculation of K_P is very direct since the normal force, spindle speed, and grinder position are measured. The threshold force, F_{TH} , has been shown to be nearly constant for all the carbon steels tested, and is treated as a constant for the subsequent experiments. Figure 4 depicts the calculated real-time grinding model coefficient, K_P , and its average value, from a force-regulated grinding experiment with 1020 steel, using data sampled at 4.5 ms. The real-time values of K_P are calculated using equation (5), and then low-pass filtered at 10 Hz to reduce noise from the numerical differentiation. The time variation of K_P is evident; indicating that a constant value is not appropriate for more precise grinding estimation. It should be noted that K_P must be positive

or zero as a value less than zero would imply that contact between the wheel and the work is lost. It should be noted that K_P depicted in the Figure also includes unmodeled tool end dynamics of the grinder in addition to the process variation.

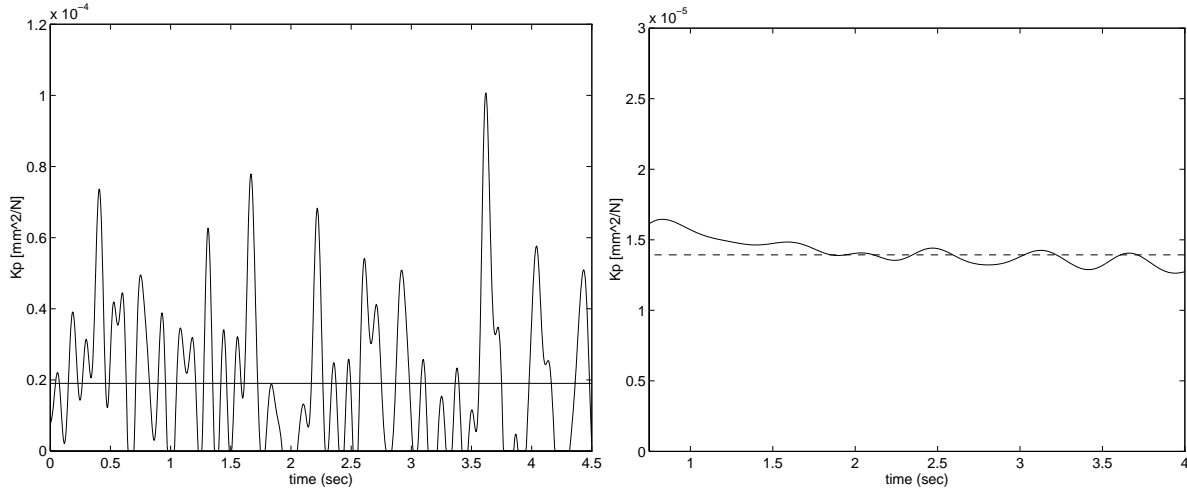


Figure 4. Real-time Coefficient, K_P , and Average K_P .

Applying the real-time values of the grinding model parameter, K_P , to simulations of an actual experiment, shows some improvements over the constant parameter case. Indeed, the simulation with the real-time K_P values shows a closer resemblance to the actual experimental data as seen in Figure 5. The lower line (in Figure 5) represents the simulated grinder displacements, while the upper line is the actual measured grinder displacement. As K_P is always positive or zero, the simulated grinder displacement curve represents the ground part surface as it only moves downward or remains constant. The real-time calculated value of K_P improves the model, however the model displacements still diverge with time. A constant filter cut-off frequency may not provide the best estimate of K_P from the noisy data.

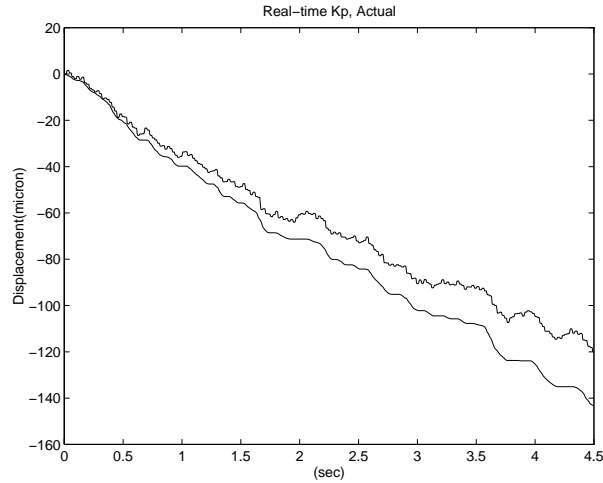


Figure 5. Simulated and Actual Displacements. The lower curve is the real-time model results, while the upper curve is the actual measured displacement data.

Multiple Sensor Estimation

Although a real-time calculation of K_P yields more accurate results for the grinder displacement than the constant parameter model, there is still a need to improve the real-time grinding model accuracy for use in adaptive force control. Estimation of K_P using multiple sensor input is a means of accomplishing this. Sensor data both directly and indirectly related to the calculation of K_P have correlations to the MRR. This is also seen in Figure 6, plotting the spindle speed, displacement, tangential and normal forces (from both the strain-gage force sensor and the PZT force sensor) for a position plunge grind of AISI-A2 carbon steel.

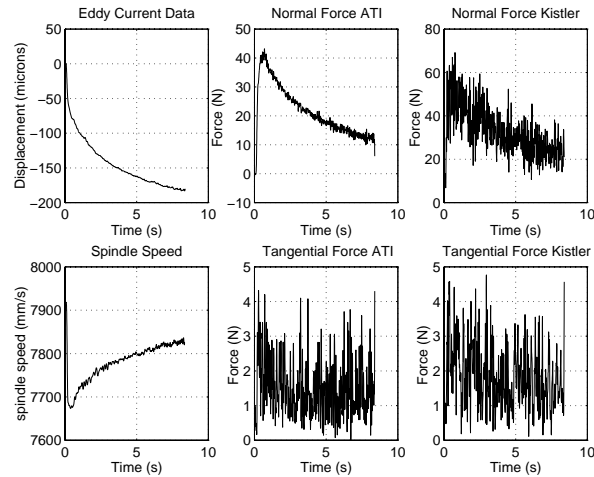


Figure 6. Typical Sensor Data and Correlation for a Step Position Plunge Grind.

It has been seen that the MRR can be correlated to several sensor values, including tangential cutting forces as well as normal forces in plunge grinding. Clearly, correlations exist for other sensory data such as wheel speed or input power. Thus, it is proposed that sensor fusion with multi-input estimation may be employed to extract and utilize potential additional information from each sensor.

The integration of multiple sensors with recursive estimation techniques can serve to improve the parameter estimate by extraction of additional information from these sensor data. This can be viewed as real-time filtering. Several recursive methods are implemented and evaluated for this task. These multi-input methods include recursive least squares with forgetting factor (RLS-FF) methods and windowed Kalman filtering. These methods are used for integrating the data streams from the two force sensors as well as the grinder spindle velocity data as inputs for grinding process parameter estimation.

Other potential methods for multi-variable input for estimation include basis functions and neural networks. The basis function (BF) method uses a series expansion in terms of a limited number of known functions that form a basis (Ljung and Soderstrom 1983). BF methods work best when the number of functions is limited and a parameter variation can be expressed in few terms. It has also been demonstrated that basis functions are not always robust, and require some prior knowledge of the parameter variation to satisfactorily represent the data set. Since the time varying response of the grinding model coefficient, K_p , is not known *a priori* it is difficult to limit the type and number of functions needed to span a basis.

Neural network approaches require no pre-determined model structure, as knowledge and relational patterns are trained into the network. A multi-level neural network structure with non-linear activations can store knowledge and attain a higher level feature abstraction. Despite all the advantages of neural networks, this approach has severe restrictions and limitations for use in real-time estimation. The number of training cases needed to bound the set of possible solutions for the grinding process parameter may not be practical (or even known) with grinding. Training data are dependent on the particular setup in grinding, and are not usually known *a priori*. Also training of a backpropagation network can take thousands of repetitions to generalize and complete learning to an acceptable error level.

Based on these factors the approaches taken for the development of real-time multi-sensor techniques to improve the estimate of the grinding model parameter are limited to the recursive techniques including a windowed Kalman filter and recursive least squares with a forgetting factor (RLS-FF). Low-pass filtering of K_p is also examined for comparison purposes.

EXPERIMENTAL GRINDING SYSTEM DESCRIPTION

An experimental platform was designed and constructed as a test-bed for performing research on real-time grinding estimation and adaptive force control. The set-up depicted in Figure 7 is nearly identical to the setup described in Jenkins and Kurfess (1995).

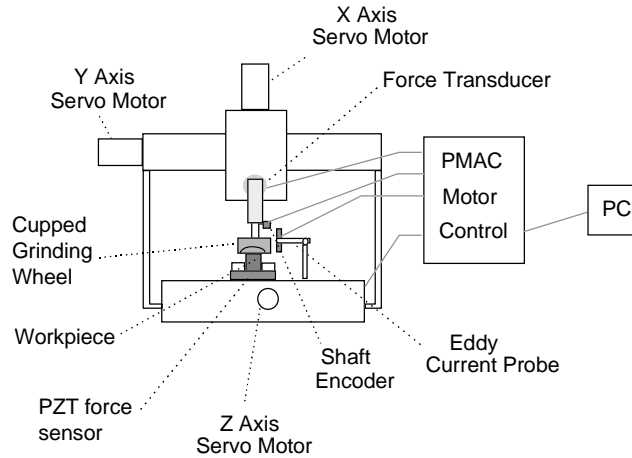


Figure 7. Experimental Grinding System Schematic.

Servo Stage

The servo stage is controlled by a PC-hosted, programmable multi-axis controller (PMAC) from Delta Tau Data Systems using a sample rate of 2.26 kHz. The controller has 16-bit analog to digital conversion capability, that permits incorporation of analog sensors. Each axis of the stage is equipped with a ball bearing lead screw driven by a DC voltage servo motor with an A/B quadrature 500-line optical shaft encoder providing a resolution of 2 μm .

Parallel Processing and Implementation

Communication between the PMAC and the host PC is accomplished by two means. The normal communication mode is via the PC-EISA bus. However, a faster mode of communication is available using the PMAC/PC dual-ported RAM, occurring within one PMAC servo cycle. Implementation of the parameter estimation routines and adaptive control algorithms is performed in real-time using this dual-processing capability of the PMAC controller with the host PC. In this implementation the PC processes the information stored in the dual-ported RAM using a fixed length data window, much smaller than the total memory. A visualization of this windowing scheme for adaptive parameter estimation and control implementation is depicted in Figure 8. As seen in Figure 8, the PC is used to determine new controller gains for the PMAC

based on the latest sensor information and estimation calculations. The new controller gains are also passed transparently to the PMAC for use in the next servo cycle via the dual-ported RAM. This arrangement allows each CPU to perform its tasks independently, unhampered by the status of the other CPU.

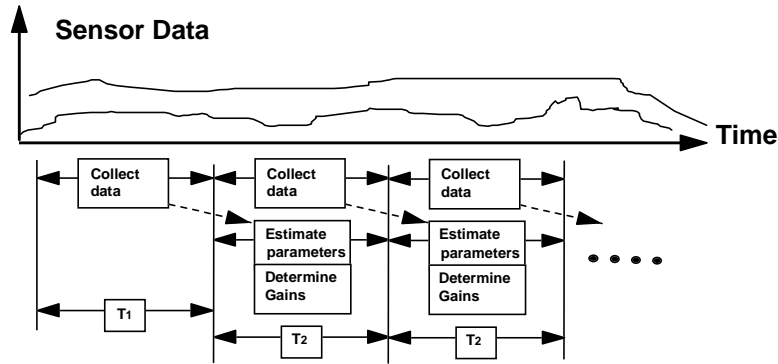


Figure 8. Windowing Scheme for Data Collection and Estimation.

The Kalman filter requires an estimate of the process and sensor noise variance in order to calculate the optimal filter gain. Recursive process statistics are calculated using discrete time windows. The covariance of the data in a previous window is used to update the Kalman gain in the following window. Thus the windowed statistics are used to determine the current state of the grinding wheel and the part. There is a trade-off in the selection of the window size. Longer windows permit better estimates of the data variances, while shorter windows contain more recent data for the current grinding condition.

The other multi-input estimation method examined in this research is the recursive least squares with a forgetting factor (RLS-FF). Here the forgetting factor, λ , serves in the same role as the window size in the Kalman filter approach. When λ approaches one, there is little forgetting and the timeliness of the data is lost, but there are smaller covariances. When λ approaches zero, the past data are quickly forgotten, so the variances of the data are very large, limiting the estimation accuracy. An “optimum” λ must be sought.

Simulations

MATLAB procedures were used to develop the recursive estimation algorithms for estimating, K_p , and simulate the material removal for the two techniques examined (RLS-FF, and windowed Kalman filtering). The sensor data from the force regulated grinding experiments are used as input to the simulations. The real-time grinding model coefficient, K_p , of equation (5), is

calculated based on these recorded sensor data. The recursive estimation techniques are then applied to this calculated real-time K_P .

The error covariance, P , between the actual grinder displacements and the simulated grinder displacements is the metric used for the numerical comparison of the different estimators. The displacement error covariances are calculated (equation 6) for the first 1,000 data points (4.5s).

$$P = \frac{1}{1,000} \sum_{k=1}^{1,000} (x_{f,k} - \hat{x}_{f,k})^2 \quad (6)$$

Kalman Filtering

First the windowed Kalman filter approach is simulated, using only one additional input, the tangential cutting force data from the strain-gage force sensor. Figure 9 depicts the estimated value of K_P and its variation from the calculated real-time value from an AISI 1020 steel experiment with a 20-point window (8.85 ms). Figure 10 plots the simulated and actual grinder displacements. The simulated displacements using Kalman filtering are greatly improved over the low-pass filtered data in Figure 5. The error covariance, equation (6), decreased from 45 to 10. From the figure, the addition of the tangential force sensor data improves the estimate of the grinding coefficient, K_P .

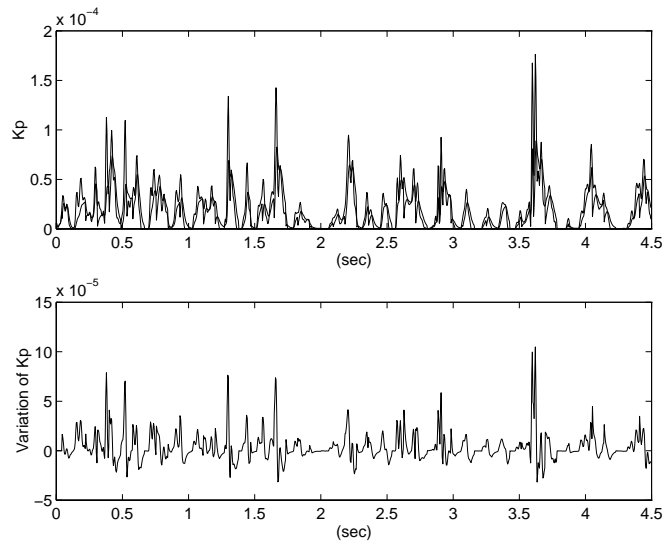


Figure 9. Real-time Coefficient (Kalman Filtered) (top) and Variation from Real-Time Calculations (bottom).

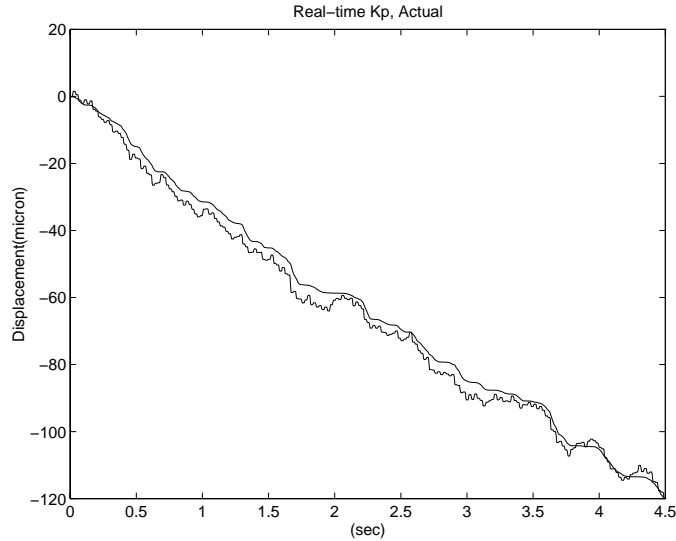


Figure 10. Simulated and Actual Displacements (Kalman Filtered).

Simulations conducted on the 1020 steel data provides some insights into the relationships of noise assignment, window size and estimation accuracy. Table 2 summarizes the effects of low-pass filtering for a representative grinding model simulation. From the data in Table 2 several issues are clear. First the improved accuracy for lower frequency filtering indicates that the significant frequency content of the K_P and the grinding process is relatively low in comparison to the system structural modes (greater than 100 Hz).

Table 2. Displacement Error Covariance.

Selected Case	Error Covariance
Constant linear K_P	45
Real-time K_P Low Pass Filtered 50 Hz	2507
Real-time K_P Low Pass Filtered 30 Hz	1180
Real-time K_P Low Pass Filtered 20 Hz	271
Real-time K_P Low Pass Filtered 10 Hz	81
Real-time K_P Low Pass Filtered 1 Hz	129

The results for the Kalman filter estimations for several materials tested using various window sizes are given in Table 3. Window sizes between 5 and 100 were examined, using a sample time of 4.45 ms. In general the Kalman filter provides a better estimate of K_P than low-pass filtering. However, the optimum window size varies to achieve the best estimate. The percentage of attributable signal variance as process noise is found to have an insignificant effect on the performance of the Kalman filter in this case.

Table 3. Error Covariance for Kalman Filter vs. Window Size.

Material	1020a	1020b	A2	O1	4142	718	8119
Low-pass filtered	2.28	159.54	42.58	54.95	1.59	19.59	23.55
Kalman filter window size							
5	27.72	964.1	367.91	1,850.	250.44	193.06	0.74
10	7.66	233.90	94.567	788.96	97.85	53.22	1.73
20	1.27	9.85	3.11	272.18	25.14	0.98	10.24
25	0.44	14.10	6.40	179.86	15.49	0.73	13.82
40	0.52	43.05	38.62	81.04	2.36	15.94	22.37
50	1.75	73.67	39.53	72.77	4.42	5.62	19.94
100	3.59	158.30	56.80	27.06	1.51	16.37	25.36

Recursive Least Squares with Forgetting

Simulations were conducted for the RLS-FF estimation method, yielding results similar to the windowed Kalman filter. Figure 11 plots the simulated and actual grinder displacements. The simulated displacements using the RLS-FF techniques also show significant improvement over the low-pass filtered data in Figure 5. The covariance error measure of equation (6-6) was 11. The effects of higher order recursive models and changing the forgetting factors were examined. A 2nd order model with $\lambda=0.8$ appears to be provide the best model result.

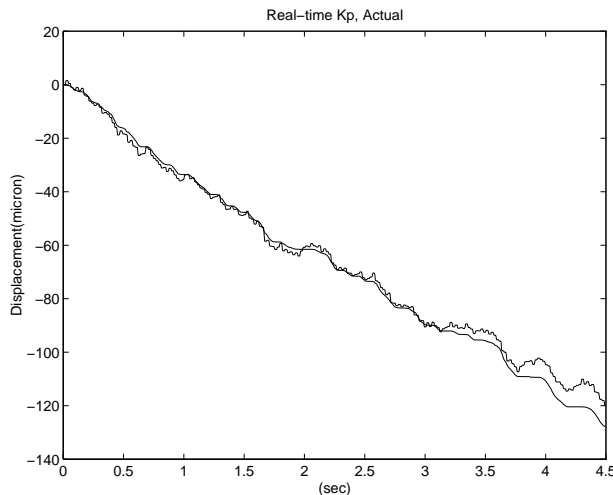


Figure 11. Simulated and Actual Displacements (2nd Order Model, RLS-FF, $\lambda=0.8$)

Simulations were also conducted for the other material specimens. The results are summarized in Table 4. Clearly the RLS-FF method overall improves the general estimation, as compared to low-pass filtering. For the particular case of AISI 4142 the error actually increased, however the

magnitude of the error is small. Thus the estimate is still very good as the real-time calculation is fairly accurate, so the increase in error is not significant. It should also be apparent that the RLS-FF method has less variation than the windowed Kalman filter. This is due to the potential divergent nature of the Kalman filter in some instances (Ydstie 1985).

Table 4. Error Covariance for RLS-FF vs. Forgetting Factor, λ

Material	1020a	1020b	A2	O1	4142	718	8119
Low-pass Filtered	2.279	159.54	42.58	54.95	1.59	19.59	23.55
λ							
0.99	0.591	43.80	20.35	354.20	16.37	5.71	2.02
0.95	0.343	16.90	14.25	123.45	9.79	5.83	0.88
0.9	0.328	14.11	13.07	98.00	9.04	4.78	0.65
0.8	0.331	21.73	11.09	71.12	7.41	3.85	0.50
0.7	0.331	25.48	9.31	65.18	7.32	3.86	0.45
0.6	0.352	27.31	9.33	59.21	7.56	3.83	0.43
0.5	0.367	28.17	9.11	58.06	7.69	3.96	0.39
0.4	0.374	28.47	9.58	58.59	7.66	3.98	0.36
0.3	0.377	28.46	9.07	57.80	7.51	3.99	0.36
0.2	0.378	28.42	8.31	57.11	7.57	4.01	0.35
0.1	0.379	28.61	7.83	56.33	7.52	4.03	0.36

Parameter Optimizations

Window size variation is examined for the effect on the displacement error covariance. The window size represents a trade-off between accuracy and timeliness of the data. If the window is too large, the data can be old and less useful; and if the window is too small the statistical variances are too large. Depending on the sensor sampling rate and the process variation spectrum, there should be a preferred sampling window balancing the timeliness of sensor data and a meaningful statistical representation of process.

There appears to be an optimum window based on the data plotted in Figure 12, depicting the relative model error covariance versus the window size for several materials examined. Note: the relative error is the model error using a particular window divided by the maximum error found for the particular material. The real-time coefficient, K_p , is determined in this case by windowed Kalman filter estimation, using the tangential strain-gage force signal as an additional sensor input. The maximum value in each case is used as a scaling factor. By examining Figure 12, it can be seen that there is not a single optimum window value for all the steels tested. However,

two data trends can be seen when the data are separated into lower and higher MRR (or lower and higher average K_p).

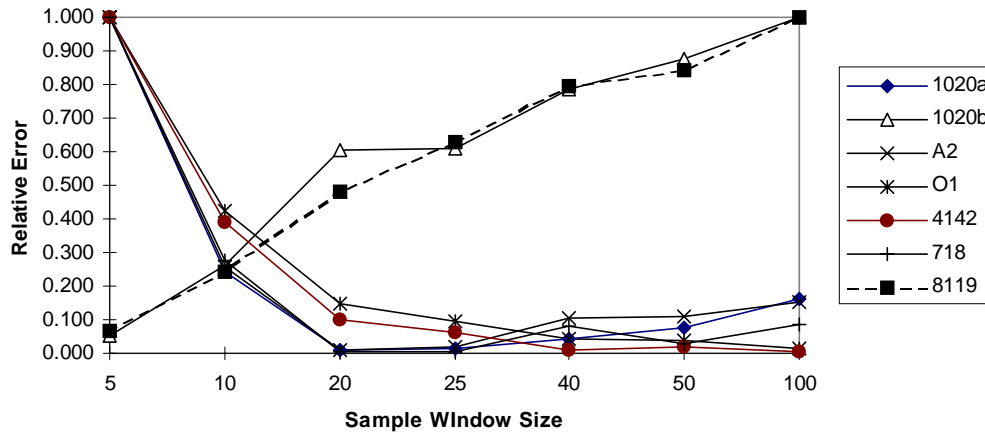


Figure 12. Windowed Kalman Filter Estimation.

The experimental cases where the grinding model error decreases with increasing window size correspond to the relatively higher material removal rates of carbon steels 1020A, A2, O1, 4142 and Inconel 718. It should be noted that two cases for 1020 carbon steel are examined. One for a newly dressed wheel, and one with a relatively dull/loaded wheel. An “optimal” window for the lower MRR cases is observed and appears to be a size range of 25-40 samples in these cases.

In cases where the model error increases with the window size, the values of K_p and the associated material removal rates are small. Thus, small movements of the grinding wheel are important so smaller windows are needed to detect and model these smaller (higher frequency) movements. The window size represents a trade-off between the timeliness of data and better data fits. Indeed, if the MRR and displacements are relatively small, then small variations are important so shorter windows are preferred. For high MRR (high K_p) the relative model error decreases with increasing window size. While for the lower MRR the converse is true; the model estimate improves with decreasing window size. For lower MRR cases, the best sampling window is 5 samples.

Similar results are seen in Figure 13 for the RLS-FF technique. In this estimation scheme larger forgetting factors are needed where small variations are important in the parameter estimation, much like the shorter windows for the windowed Kalman filter. Again there is not a single optimum forgetting factor. Lower MRR cases have smaller model error when the forgetting

factor (FF) is closer to 1.0, while higher MRR cases have the best estimates with FF values from 0.9 to 0.6.

It should be noted that the RLS-FF approach yields similar results to the windowed Kalman filter. However for implementation the RLS-FF technique is preferred over the Kalman filter. The Kalman filter with multiple input requires a calculation intensive matrix inversion, while the recursive RLS method does not. Thus all further experiments, simulations, and implementation concentrate on the RLS-FF technique.

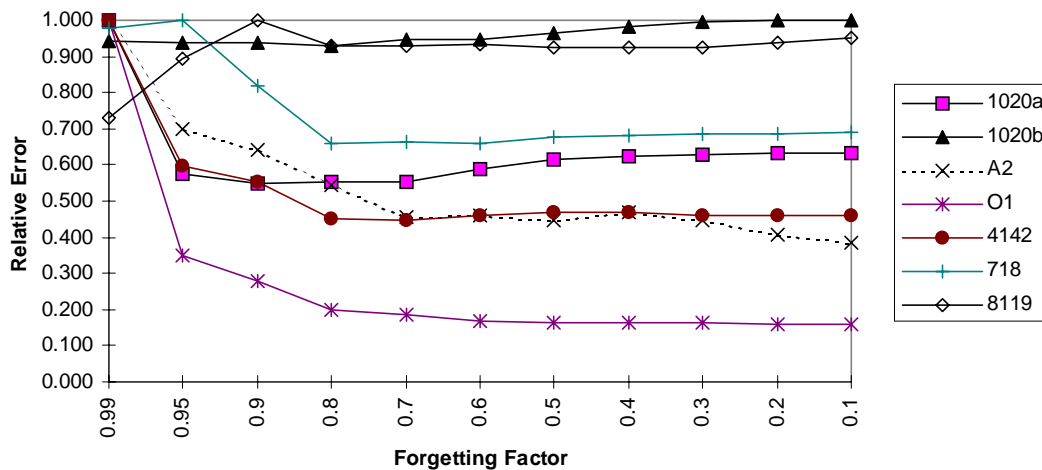


Figure 13. RLS with Forgetting Factor Estimation.

Input Sensor Effects on Estimation

It was proposed that by adding more related sensor data into the estimation scheme additional improvement would be seen. To this end, estimations using the various sensor combinations are simulated using the RLS algorithm with a forgetting factor of 0.6. An analysis of the effects of additional sensor data used in parameter estimation is presented in Figure 14. Note: FT and FN are the tangential and normal forces from the strain gage sensor, FT2 and FN2 are the tangential and normal forces from the PZT sensor. W is the grinder spindle speed.

Figure 14 plots the error covariance of several sensor configurations, relative to a base case of one tangential force sensor as additional input data to the RLS algorithm. Three lines represent the average of all materials, a softer steel (A2 carbon steel) and the hardest steel tested (8119 case hardened). From these data depicted in Figure 14, it can be seen that indeed some improvement can be gained with additional sensor information. However, the additional information does not always reduce the model error, from the nominal case of using only the strain gage tangential

force as additional input. The best single case improvement was a 37% reduction, while the worst single case was a 27% increase in the error. It appears that using all the available sensor data provides the most improvement in parameter estimation. The best average result obtained using all available sensor input, was an improvement of 7%. It is also interesting to note that the PZT sensor signals showed the most improvement for the hardest material examined (AISI 8119), again indicating that higher frequency information is important in low MRR cases.

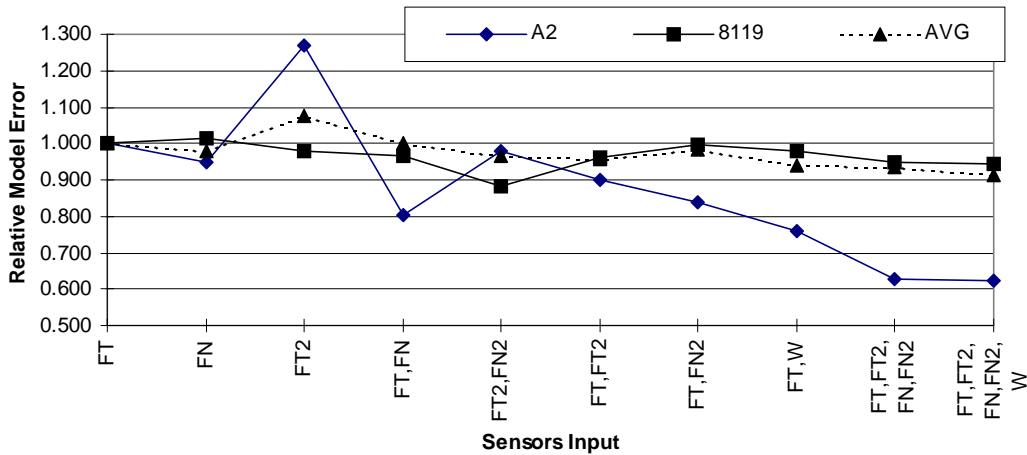


Figure 14. Relative Model Error for Various Sensor Inputs.

DISCUSSION AND CONCLUSIONS

Separation of the process dynamics from the structural vibrations is effectively accomplished by low-pass filtering of the real-time calculation of the coefficient K_p . A frequency analyzer revealed that the primary structural response of the servo grinding system is higher than 100 Hz. However, there are still some unmodeled system dynamics that are present in K_p . A clear improvement is seen in the model prediction when low-pass filtering the coefficient, K_p . Low-pass filtering at lower cut-off frequencies produces better accuracy, until approximately 1 to 10 Hz. This is reasonable as the bandwidth of the position controller is nominally 36 Hz. From this it is apparent that grinding process variation is generally of a lower frequency spectrum than the servo structure.

Several recursive techniques including a windowed Kalman filter and recursive least squares with a forgetting factor (RLS-FF) yielded excellent improvements in estimating the grinding model coefficient over conventional low-pass filtering alone. Integration of additional sensors

for estimation of the model coefficient was successfully demonstrated through simulations using actual experimental grinding data.

It is interesting to note that the RLS-FF method and windowed Kalman filter method yielded similar results for the real-time grinding model accuracy. This is not unexpected as both are rooted in the general least-squares estimation approach.

Both the windowed Kalman filter and the RLS-FF methods have a parameter related to the timeliness of the data. These are time weighting parameters for emphasizing the frequency content of the sensor data to be considered. Further examination of these parameters provided a basis for their selection, based on the best performance of the model.

The tested materials can be divided into two groups based on the relative MRR and average K_p . This distinction between higher and lower MRR is of course relative to the sampling rate of the estimator. From the data depicted in Figures 12 and Figure 13, it can be seen that there is not a single value that provides the optimum window or forgetting factor for all of the steels tested. In examining the Kalman filtering results for higher MRR cases (high average K_p), the relative model error decreases with increasing window size and for the lower MRR the converse is true. The “best” window size for the higher MRR cases is observed and appears to be in the range of 25-40 samples, and is specific for the material tested and the sampling time. For the lower material removal rate materials, shorter windows are required to detect the finer movements of the grinding wheel. For lower MRR cases, the smaller sampling window sizes provided the lowest model error.

The RLS-FF approach yielded similar results to the windowed Kalman filter. In the RLS-FF estimation, larger forgetting factors are needed where small variations are important to the parameter estimation, much like the shorter windows for the Kalman filter. Lower MRR cases have smaller model error when the forgetting factor (FF) is closer to 1.0, while higher MRR cases have the best estimates with FF values from 0.9 to 0.6. Again there is no single optimum forgetting factor, as the best choice is dependent on the processing materials and sampling time.

The window size for the Kalman filter is related to the forgetting factor in the RLS-FF approach. This is obvious from the trends in the plots of relative error vs. window size in Figure 6-18 and relative error vs. forgetting factor in Figure 6-19. For the example case of 1020 steel the smallest relative model error is obtained for a 25 data point sampling window with a Kalman filter, while the best forgetting factor is about 0.8. In examining the RLS-FF approach, the effect of a data point from 25 sample periods past may be approximately considered as $(0.8)^{25}$. This value is less than 0.01, so its contribution to the RLS estimation is small, if not negligible. This is consistent with the window size of the Kalman filter showing no benefit to error reduction after

approximately 20 to 25 sample periods. From the plots it is easily seen that the forgetting factor is directly correlated to the Kalman filter window size for each test case, although a closed-form relation was not examined.

It was proposed that by adding more related sensor data into the estimation scheme, real-time model improvement would be seen. From the data depicted in Figure 6-20, it can be seen that indeed some improvement can be gained by using additional sensor signals for input. However, the additional information does not always reduce the model error, compared to the nominal case of using only the strain gage tangential force as additional input. The various sensor combinations yielded mixed results, as compared to the nominal case. The best single case improvement was a 37% error reduction, while the worst single case was a 27% increase in the error. Using all the available sensor data provided the most improvement in estimation, which was 8% for an average result.

Clearly it seems for industrial systems that extensive measuring and use of sensor signals is not needed. In general the addition of the force signal alone was sufficient to improve the filtering of the model coefficient. This was not unexpected as all the sensor signals exhibit correlation to the MRR. There is less benefit gained as additional sensors are added. However, the use of additional sensors does provide fault tolerance.

A major contribution of this work is the demonstration that the grinding process is a time-varying process, best modeled in real-time. The process dynamics, represented in K_p , have been shown to be of frequency range of 1 to 10-Hz, which is significantly lower than the most grinder structures. Previous research in grinding has viewed it as a nominally constant process. As a result of the observation of the time-varying nature of grinding, the first real-time implementation of model-based, adaptive estimation and process control to grinding has been successfully developed in this thesis (to the author's knowledge). This has been accomplished using several adaptive, multiple input estimation methods for determining the grinding model coefficient, K_p . In this approach the integration of multiple sensor data achieved a superior grinding model parameter estimation, suitable for adaptive control of the normal grinding force.

Future Work

Future research should include investigating the validity of the two-parameter grinding model to other metals and alloys as well as non-metallic materials such as ceramic and glass. For industrial applications the process-specific attributes must be examined to determine the appropriate model parameters necessary for successful application of the process control approach. Factors such as workpiece material, grinding wheel properties (bond, grits), dressing, coolants, sampling times, etc., must be considered as evident from the results obtained for the

different steels studied. Also the estimation algorithm, could be used to detect excess wheel dulling and provide for automatic redressing, as needed.

Lastly, there appears a potential to expand the application of multi-sensor estimation technology to other areas for improved real-time model estimation and process control.

BIBLIOGRAPHY

Astrom, K. J. and Wittenmark, B., *Adaptive Control*, Addison-Wesley Publishing Co., Reading MA, 1989.

Coes, L., *Abrassives*, Springe-Verlag, New York, 1971.

Danai, K. and Ulsoy, A. G., "An Adaptive Observer for On-Line Tool Wear Estimation in Turning, Part I and Part II," *Mechanical Systems and Signal Processing*, 1987, Vol. 1, No. 2, pp. 211-240.

Franklin, G. F., Powell, J. D., and Workman, M. L., *Digital Control of Dynamic Systems*, Addison-Wesley, Reading, MA, Second Edition, 1990.

Hahn, R. S. and Lindsay, R. P. "Principles of Grinding Part I Basic Relationships in Precision Machining," *Machinery*, July 1971, pp. 55-62.

Jenkins, H.E., Kurfess, T.R., and Ludwick, S.J., "Determination of a Dynamic Grinding Model," (accepted February 1996) *ASME Journal of Dynamic Systems, Measurement and Control*.

Lewis, F.L., *Optimal Estimation*, John Wiley and Sons, New York, 2nd Ed., 1992.

Ljung, L. and Soderstrom, T., 1983, *Theory and Practice of Recursive Identification*, MIT Press Cambridge MA.

Ljung, L., *System Identification: Theory for the User*, Prentice Hall, Englewood Cliffs, NJ, 1987.

Malkin, S., *Grinding Technology , Theory and Applications of Machining with Abrasives*, Ellis Horwood Limited,Chichester, U.K., 1989.

Park, J. and Ulsoy, A. G., "On-Line Flank Wear Estimation Using an Adaptive Observer and Computer Vision, Part 1: Theory," *ASME Journal of Engineering for Industry*, 1993, Vol. 115, pp. 30-36.

Tonshoff, H. K., Zinngrebe, M., Kemmerling, M., "Optimization of Internal Grinding by Microcomputer-Based Force Control," *Annals of the CIRP*, Vol. 35, No. 1, 1986, pp. 293-6.

Ydstie, B. E., Co, T., "Recursive Estimation with Adaptive Divergence Control," *IEE Proceedings, Part D: Control Theory and Applications*, Vol. 132, No. 3, 1985, pp. 124-130.